



# Acute myeloid leukemia sensitivity to metabolic inhibitors: glycolysis showed to be a better therapeutic target

Beatriz Lapa<sup>1,2</sup> · Ana Cristina Gonçalves<sup>1,2,3,4</sup> · Joana Jorge<sup>1,2,3,4</sup> · Raquel Alves<sup>1,2,3,4</sup> · Ana Salomé Pires<sup>2,3,4,5</sup> · Ana Margarida Abrantes<sup>2,3,4,5</sup> · Margarida Coucelo<sup>2,3,4,6</sup> · Antero Abrunhosa<sup>7</sup> · Maria Filomena Botelho<sup>2,3,4,5</sup> · José Manuel Nascimento-Costa<sup>2,3,4,8</sup> · Ana Bela Sarmiento-Ribeiro<sup>1,2,3,4,6</sup>

Received: 7 April 2020 / Accepted: 16 July 2020 / Published online: 28 July 2020  
© Springer Science+Business Media, LLC, part of Springer Nature 2020

## Abstract

Cancer cells alter their metabolism by switching from glycolysis to oxidative phosphorylation (OXPHOS), regardless of oxygen availability. Metabolism may be a molecular target in acute myeloid leukemia (AML), where mutations in metabolic genes have been described. This study evaluated glycolysis and OXPHOS as therapeutic targets. The sensitivity to 2-deoxy-D-glucose (2-DG; glycolysis inhibitor) and oligomycin (OXPHOS inhibitor) was tested in six AML cell lines (HEL, HL-60, K-562, KG-1, NB-4, THP-1). These cells were characterized for *IDH1/2* exon 4 mutations, reactive oxygen species, and mitochondrial membrane potential. Metabolic activity was assessed by resazurin assay, whereas cell death and cell cycle were assessed by flow cytometry. Glucose uptake and metabolism-related gene expression were analyzed by <sup>18</sup>F-FDG and RT-PCR/qPCR, respectively. No *IDH1/2* exon 4 mutations were detected. HEL cells had the highest <sup>18</sup>F-FDG uptake and peroxides/superoxide anion levels, whereas THP-1 showed the lowest. 2-DG reduced metabolic activity in all cell lines with HEL, KG-1, and NB-4 being the most sensitive cells. Oligomycin decreased metabolic activity in a cell line-dependent manner, the THP-1 resistant and HL-60 being the most sensitive. Both inhibitors induced apoptosis and cell cycle arrest in a cell line- and compound-dependent manner. 2-DG decreased <sup>18</sup>F-FDG uptake in HEL, HL-60, KG-1, and NB-4, while oligomycin increased the uptake in K-562. Metabolism gene expression had different responses to treatments. In conclusion, HEL and KG-1 show to be more glycolytic, whereas HL-60 was more OXPHOS dependent. Results suggest that AML cells reprogram their metabolism to overcome OXPHOS inhibition suggesting that glycolysis may be a better therapeutic target.

**Keywords** Therapeutic target · Acute myeloid leukemia · Glycolysis · Oxidative phosphorylation · 2-Deoxy-D-glucose · Oligomycin

**Electronic supplementary material** The online version of this article (<https://doi.org/10.1007/s12032-020-01394-6>) contains supplementary material, which is available to authorized users.

✉ Ana Cristina Gonçalves  
acgoncalves@fmed.uc.pt

<sup>1</sup> Faculty of Medicine (FMUC), Laboratory of Oncobiology and Hematology (LOH) and University Clinic of Hematology, University of Coimbra, Azinhaga de Santa Comba-Celas, 3000-548 Coimbra, Portugal

<sup>2</sup> Coimbra Institute for Clinical and Biomedical Research (iCBR) - Research Area of Environment Genetics and Oncobiology (CIMAGO), FMUC, University of Coimbra, Coimbra, Portugal

<sup>3</sup> Clinical Academic Center of Coimbra, CACC, Coimbra, Portugal

<sup>4</sup> Center for Innovative Biomedicine and Biotechnology (CIBB), University of Coimbra, Coimbra, Portugal

<sup>5</sup> Faculty of Medicine (FMUC), Biophysics Unit, University of Coimbra, Coimbra, Portugal

<sup>6</sup> Clinical Hematology Department, Centro Hospitalar Universitário de Coimbra (CHUC), Coimbra, Portugal

<sup>7</sup> Institute of Nuclear Sciences Applied to Health (ICNAS), University of Coimbra, Coimbra, Portugal

<sup>8</sup> Faculty of Medicine (FMUC), University Clinic of Oncology, University of Coimbra, Coimbra, Portugal

## Introduction

Since the mid-twentieth century, it has been known that cancer cells show characteristic alterations in their metabolic activity to sustain high levels of growth and proliferation [1, 2]. Otto Warburg and co-workers showed that, under aerobic conditions, tumor tissues metabolize glucose to lactate approximately tenfold more than normal tissue [3, 4]. This metabolic rewiring is the most ubiquitous and best characterized metabolic phenotype seen across cancer cells and was termed as the Warburg effect or aerobic glycolysis [4, 5]. The catabolism of glucose into lactate can produce ATP faster, but is far less efficient than oxidative phosphorylation (OXPHOS), generating a considerably lesser amount of ATP (2 vs. 36 molecules of ATP per one molecule of glucose) [1, 4]. Hence, this metabolic shift is associated with various alterations in the cell that must be tightly regulated [4, 6]. Although aerobic glycolysis plays a crucial role in cancer metabolism, most tumors retain the capacity for OXPHOS or use both glycolysis and OXPHOS [3, 7]. Therefore, although glycolysis is a feature of several tumors and is associated with faster growth, active OXPHOS is also an important feature of tumors, in particular, quiescent subpopulations of tumor cells [8].

The metabolic reprogramming of tumor cells is controlled by intrinsic genetic changes, such as loss of tumor suppressors or oncogenes activation, and external responses to tumor microenvironment, like hypoxia [6]. Hypoxia-inducible factor 1 (HIF-1 $\alpha$ ), MYC, and p53 are considered to be primarily responsible for a coordinated shift from OXPHOS to glycolysis [7, 9]. HIF-1 $\alpha$  facilitates this phenotypic shift by increasing the expression of glucose transporters (particularly GLUT1 and GLUT3), glycolytic enzymes, such as hexokinase (HK) and pyruvate dehydrogenase kinase [6, 10]. MYC cooperates with HIF-1 $\alpha$  in activating several genes that encode glycolytic proteins, but also activates the transcription of targets that increase mitochondrial biogenesis and mitochondrial function, thus stimulating OXPHOS, and is also the principal driver of glutamine uptake and glutaminolysis [6]. GLUTs, encoded by *solute carrier family 2 (SLC2A)* genes, glycolytic enzymes (such as HK), and mitochondrial metabolic enzymes [such as isocitrate dehydrogenase (IDH)], are also affected by oncogenic mutations, being associated with metabolic remodeling [3, 6, 11]. HKs are enzymes that participate in glycolysis by converting glucose to glucose-6-phosphate, thus trapping glucose inside cells [12]. IDHs convert isocitrate to  $\alpha$ -ketoglutarate ( $\alpha$ KG) in the tricarboxylic acid cycle, producing NADH or NADPH [6, 8]. There are 3 IDH isoenzymes in mammalian cells, with IDH1 and IDH2 being highly homologous

and structurally and functionally distinct from IDH3 [6, 8]. Mutant IDH1/2 exhibits an oncogenic gain of function by converting  $\alpha$ KG into 2-hydroxyglutarate that functions as an oncometabolite and leads to a shift from NADPH production to NADPH consumption [6, 8]. Mutations in *IDH1/2* have been detected in 15–20% of all acute myeloid leukemia (AML) patients, which could indicate the existence of a metabolic reprogramming in AML cells [13, 14].

AML is a heterogeneous clonal disorder of hematopoietic progenitor cells characterized by a block in myeloid differentiation and uncontrolled proliferation of abnormal myeloid progenitors that accumulate in the bone marrow and, later, in blood [13, 15]. Despite the research that has been carried out to find new prognostic biomarkers and treatments, AML still has a variable prognosis and a high mortality rate [13]. Therefore, increased knowledge of AML pathophysiology could lead to finding new biomarkers and therapeutic approaches [16]. Targeting glycolysis has become progressively attractive as a therapeutic approach since it is a relatively unique metabolism in cancer cells [17]. However, it is not yet entirely clear how dependent leukemia cells are on glycolysis and/or OXPHOS and which leukemia cells are more sensitive to these pathways' inhibition. In this study, we aimed to analyze some metabolic features of several AML cell lines and study the potential of metabolism, namely, glycolysis and OXPHOS, as therapeutic targets, using in vitro models of AML.

## Materials and methods

### Cell culture

AML cell lines HEL, HL-60, K-562, KG-1, and THP-1 were purchased from American Type Culture Collection (ATCC) and NB-4 from the German Collection of Microorganisms and Cell Cultures (DSMZ). These cells were cultured in Roswell Park Memorial Institute 1640 medium (RPMI-1640) supplemented with 10% heat-inactivated fetal bovine serum (FBS; Gibco, Invitrogen), 2 mM of L-glutamine, 100 U/mL of penicillin, and 100  $\mu$ g/mL of streptomycin (Gibco, Invitrogen). Cells were grown at an initial density of 0.3 (HL-60), 0.4 (HEL and NB-4), or 0.5 (K-562, KG-1, and THP-1)  $\times 10^6$  cells/mL. Cell lines were incubated in the absence and presence of increasing doses of 2-Deoxy-D-Glucose (2-DG—glycolysis inhibitor; APExBIO) and oligomycin complex (Oligo—OXPHOS inhibitor; APExBIO) for different periods of time depending on the assay. 2-DG was prepared in water and oligomycin in dimethyl sulfoxide (DMSO).

## Reactive oxygen species (ROS) levels and mitochondrial membrane potential assessment

ROS levels (intracellular peroxides and superoxide anion) and mitochondrial membrane potential ( $\Delta\psi_{mit}$ ) were measured by fluorometric assays using 2',7'-dichlorodihydrofluorescein diacetate (DCFH<sub>2</sub>-DA; Molecular Probes, Invitrogen), dihydroethidium (DHE; Sigma-Aldrich), and 5,5',6,6'-tetrachloro-1,1',3,3'-tetraethylbenzimidazolcarbocyanine iodide (JC-1; Molecular Probes, Invitrogen) probes, respectively. Briefly, 50,000 cells were collected and washed with phosphate-buffered saline (PBS) by centrifugation for 5 min at 300×g. Afterward, cells were resuspended in PBS, incubated at 37 °C, and protected from light for 45 min with 2 μM of DCFH<sub>2</sub>-DA and for 15 min with 4 μM of DHE or 5 μg/mL of JC-1. Cells were then washed and resuspended in PBS. Fluorescence readings at emission wavelength of 525 nm for DCFH<sub>2</sub>-DA, 620 nm for DHE, and 590/525 nm for JC-1 were performed on a microplate spectrophotometer (Synergy™ HT Multi-Mode Microplate Reader, BioTek Instruments). The results were expressed in fluorescence intensity (FI, arbitrary units) and represent mean ± standard error of the mean (SEM) of five independent experiments. For JC-1, results represent aggregates/monomers ratio of five independent experiments.

## Isocitrate dehydrogenases exon 4 mutations assessment

Mutations in the exon 4 of *IDH1* and *IDH2* genes were identified by Sanger sequencing. DNA extraction was performed using TripleXtractor (GRiSP) according to the manufacturer's protocol. *IDH1* exon 4 mutations were carried out using the following primer sequences: forward, 5'-CCATCA CTGCAGTTGTAGGTT-3' and reverse, 5'-GCAAAATCA CATTATT GCCAAC-3', and the *IDH2* exon 4 mutations were carried out using forward, 5'-GCTGCAGTGGGAC CACTATT-3' and reverse, 5'-AGTCTGTGGCCTTGTACT GCA-3'. Products were sequenced using the ABI PRISM 3500 Genetic Analyzer (Applied Biosystems).

## Metabolic activity assay

The resazurin assay was used to assess the metabolic activity of cells treated with 2-DG or oligomycin for 72 h. At every 24 h of incubation, resazurin (Sigma-Aldrich) was added to the cells, which were then incubated at 37 °C (final concentration of 10 μg/mL). The absorbance readings at 570 nm and 600 nm wavelengths were performed on a microplate spectrophotometer, and metabolic activity was calculated as

a percentage of control cells. The results were expressed as mean ± SEM of five independent experiments.

## Cell death analysis

Cell death was evaluated by flow cytometry (FC), using annexin V (AV) and 7-amino-actinomycin D (7-AAD) double staining, and by morphological analysis using optic microscopy. After an incubation period of 2 h and 24 h in absence or presence of 5 mM of 2-DG and 5 μg/mL of oligomycin, 0.5 × 10<sup>6</sup> cells were collected. Afterward, cells were washed with PBS, centrifuged at 1000×g for 5 min, resuspended in 100 μL of binding buffer, and incubated with 5 μL of AV (Biolegend) and 2 μL of 7-AAD (Biolegend) for 15 min in the dark at room temperature. Subsequently, cells were diluted in 400 μL of binding buffer, and the analysis was run on a FACSCanto flow cytometer (Becton Dickinson). Through FACS DIVA™ software, 50,000 cells were acquired and data were analyzed using Infinicyte™ software. Results represent the percentage of each cell population: viable (AV<sup>-</sup>/7-AAD<sup>-</sup>), early apoptotic (AV<sup>+</sup>/7-AAD<sup>-</sup>), late apoptotic/necrotic (AV<sup>+</sup>/7-AAD<sup>+</sup>), and necrotic cells (AV<sup>-</sup>/7-AAD<sup>+</sup>); results represent the mean ± SEM of five independent experiments. For morphological analysis, cells from the different conditions were collected and seeded in glass slides. The smears were stained and analyzed as described by Jorge et al. [18]. Cell morphology was analyzed by light microscopy using a Nikon Eclipse 80i microscope equipped with a Nikon Digital Camera DXM 1200 F.

## Cell cycle analysis

Cell cycle analysis was performed by FC, using propidium iodide/RNase cell cycle analysis kit (Immunostep), in 1 × 10<sup>6</sup> cells after 2 h and 24 h of growth in absence or exposure to 2-DG (5 mM) and oligomycin (5 μg/mL). The protocol was performed as described in Jorge et al. [18]. Cells were then analyzed on a FACSCalibur flow cytometer (Becton Dickinson) and cell cycle distribution using ModFit<sup>LT</sup> software (Verity Software House). Results were expressed as percentage of cells in the different cell cycle phases (Sub-G<sub>1</sub>, G<sub>0</sub>/G<sub>1</sub>, S, and G<sub>2</sub>/M) and represent the mean ± SEM of five independent experiments.

## <sup>18</sup>F-FDG uptake studies

Cell lines were cultured, for 2 h and 24 h, in absence or presence of 2-DG (5 mM) and oligomycin (5 μg/mL) according to Brito et al. [19]. Briefly, after this period, the medium was removed by centrifugation and cells were resuspended in new medium and incubated with <sup>18</sup>F-FDG for 5, 30, 60, 90, and 120 min. Then, cells were centrifuged (5600×g for 1 min) to separate the pellet from the supernatant. At the end

of the experiments, cell viability was determined by trypan blue exclusion method. The radioactivity of the two fractions (pellet and supernatant) was measured in a well counter (Capintec, Inc. CRC-15W) in counts per minute (CPM) in order to determine the  $^{18}\text{F}$ -FDG uptake percentage. Data represent the  $^{18}\text{F}$ -FDG uptake percentage mean  $\pm$  SEM of five independent experiments.

### Gene expression analysis

Cell lines were incubated in the absence or presence of 5 mM of 2-DG and 5  $\mu\text{g}/\text{mL}$  of oligomycin for 2 h and 24 h. Total RNA was extracted using TripleXtractor (GRiSP) and converted to cDNA using Xpert cDNA Synthesis Mastermix (GRiSP), according to the manufacturer's protocol. Gene expression of 8 *SLC2A*, 2 *HK*, and *HIF-1 $\alpha$*  was evaluated by RT-PCR (GRS Taq DNA polymerase, GRiSP) in a T100 thermal cycler (Bio-rad) and qPCR (Xpert Fast SYBR, GRiSP) in a QuantStudio™ 3 System (ThermoFisher Scientific), using *hypoxanthine phosphoribosyltransferase (HPRT)* as an endogenous control gene. Primer sequences are described in Supplemental Table S1. RT-PCR results represent the most representative image of three independent experiments. Relative gene expression was calculated using the  $2^{-\Delta\Delta\text{Ct}}$  formula. The results represent the fold change mean  $\pm$  SEM of five independent experiments.

### Statistical analysis

The statistical analysis was performed in GraphPad Prism 7 software (version 7.04 for Windows; GraphPad Software, Inc., San Diego, CA, USA). To calculate the half-maximal inhibitory concentration ( $\text{IC}_{50}$ ), a nonlinear logistic regression was applied to the data concerning the exposure of cells at 24 h. Statistical significance was determined using a non-parametric test, Kruskal–Wallis test, followed by a post hoc test, the Dunn's multiple comparison test. A significance

level of  $p < 0.05$  was considered statistically significant. Data were expressed as mean  $\pm$  SEM of the number of independent experiments (indicated in the figure legends).

## Results

### Metabolic features of AML cell lines

To assess the glucose uptake profile of different cell lines,  $^{18}\text{F}$ -FDG radiopharmaceutical uptake was evaluated. As shown in Table 1, THP-1 cell line presented the lowest  $^{18}\text{F}$ -FDG uptake percentage ( $p = 0.0001$  vs. HEL). In contrast, HEL cells showed the highest uptake percentage being, at 120 min, 3.8-fold higher than THP-1 and twofold higher than K-562 and KG-1 ( $p = 0.0266$  vs. HEL) cells. HL-60 and NB-4 presented similar values, with an uptake 2.5-fold higher than THP-1 cells. Since oxidative stress has been implicated in the growth and death of cancer cells, basal levels of peroxides and superoxide anion were assessed, as well as  $\Delta\Psi_{\text{mit}}$ . The highest levels of intracellular peroxides were observed in the HEL cell line followed by K-562, while the lowest was detected in NB-4 ( $p = 0.0001$  vs. HEL and  $p = 0.0049$  vs. K-562). HL-60 and THP-1 ( $p = 0.0236$  vs. HEL) cells presented similar and intermediate values of intracellular peroxides. HEL cell line also showed the highest levels of superoxide anion. In contrast, HL-60 and K-562 had similarly low levels of anion superoxide (HL-60:  $p = 0.0221$ ; K-562:  $p = 0.0079$  vs. HEL). KG-1, NB-4, and THP-1 presented similar and intermediate values. The  $\Delta\Psi_{\text{mit}}$  levels were similar between the tested cell lines; however, THP-1 showed the lowest aggregate/monomer ratio, while HL-60 had the highest. A higher aggregate/monomer ratio is associated with a more polarized mitochondria.

The presence of mutations in exon 4 of *IDH1/IDH2* genes were also assessed (Table 1). No mutations were found in any cell line. However, HEL, HL-60, K-562, and

**Table 1**  $^{18}\text{F}$ -FDG uptake, intracellular peroxides and superoxide anion levels, mitochondrial membrane potential ( $\Delta\Psi_{\text{mit}}$ ), and *IDH1/IDH2* exon 4 genetic analysis in HEL, HL-60, K-562, KG-1, NB-4, and THP-1 cell lines

	HEL	HL-60	K-562	KG-1	NB-4	THP-1
$^{18}\text{F}$ -FDG uptake (%)	4.6 $\pm$ 0.2	3.1 $\pm$ 0.2 <sup>#</sup>	2.4 $\pm$ 0.2	2.2 $\pm$ 0.1*	3.0 $\pm$ 0.3	1.2 $\pm$ 0.1***
Peroxides (FI)	6981 $\pm$ 132	3649 $\pm$ 28	6138 $\pm$ 158 <sup>SS</sup>	4130 $\pm$ 231	1771 $\pm$ 52***	3634 $\pm$ 104*
Superoxide anion (FI)	407.4 $\pm$ 6.8	353.3 $\pm$ 7.9*	348.4 $\pm$ 10.4**	380.2 $\pm$ 3.2	372.9 $\pm$ 6.0	377.3 $\pm$ 12.8
$\Delta\Psi_{\text{mit}}$ (ratio aggregate/monomer)	3.7 $\pm$ 0.1	4.1 $\pm$ 0.3	3.5 $\pm$ 0.4	3.3 $\pm$ 0.7	3.8 $\pm$ 0.5	3.2 $\pm$ 0.3
<i>IDH1</i> exon 4	rs11554137	rs11554137	rs11554137	rs11554137	Wt	Wt
<i>IDH2</i> exon 4	Wt	Wt	Wt	Wt	Wt	Wt

$^{18}\text{F}$ -FDG uptake data were obtained at 120 min and are expressed in percentage (%) and represent mean  $\pm$  SEM of 5 independent experiments. Intracellular peroxides and superoxide anion levels and  $\Delta\Psi_{\text{mit}}$  results are expressed in fluorescence intensity (FI, in arbitrary units) and represent mean  $\pm$  SEM from 5 independent experiments. Statistical analyses were performed using Dunn's multiple comparisons test. rs11554137, c.315C > T (p.Gly105=); Wt, wild type

\* $p < 0.05$ , \*\* $p < 0.01$ , and \*\*\* $p < 0.001$  (comparison with HEL); <sup>#</sup> $p < 0.05$  (comparison with THP-1); <sup>SS</sup> $p < 0.01$  (comparison with NB-4)



KG-1 cells have a single nucleotide variant in *IDH1* exon 4 (rs11554137), representing a C to T transversion at nucleotide 315 [c.315C>T (p.Gly105=)]. The basal expression of glucose metabolism-related genes (*SLC2A* and *HK*) and genes involved in the metabolic regulation (*HIF-1α*) were evaluated by RT-PCR. As shown in Fig. 1, not only different cell lines expressed different genes, but also, within each gene, some cell lines presented higher basal expression levels than others. THP-1 cells showed the highest expression levels of the tested genes, whereas HL-60 had the lowest (Supplemental Fig. 1).

**2-DG and oligomycin reduced metabolic activity in AML cell lines**

Our results showed a decrease in metabolic activity in time-, dose-, and cell line-dependent manner when cells

were treated with 2-DG (Fig. 2a). After 24 h of incubation, THP-1 and HL-60 cells required the highest concentration of 2-DG, presenting an IC<sub>50</sub> of 9.5 and 9.2 mM, respectively. K-562 cell line required a concentration of 6.5 mM of 2-DG to achieve a metabolic inhibition of 50%. HEL and NB-4 cell lines presented similar IC<sub>50</sub> values of 5.2 and 5.1 mM, respectively. At this time point, KG-1 cells were the most sensitive to glycolysis inhibitor, presenting an IC<sub>50</sub> of 3.7 mM. However, after 72 h of exposure to 2-DG, HEL, and NB-4 cell lines, as well as KG-1, presented the lowest values of metabolic activity. Interestingly, although an initial reduction of cell metabolic activity in K-562 and NB-4 cells has been observed with lower concentrations of 2-DG (1 and 2.5 mM), their effect was reversed after 48 h (K-562) and 72 h (NB-4). Oligomycin treatment reduced metabolic activity in a time- but mainly in a cell line-dependent manner (Fig. 2b). At tested concentrations, THP-1 cells did not show sensitivity to oligomycin since there was no reduction in metabolic activity, showing an estimated IC<sub>50</sub>, at 24 h, of 44.8 μg/mL. The IC<sub>50</sub> of KG-1 and NB-4 was equal (6.4 μg/mL). HEL and HL-60 had an IC<sub>50</sub> of 6.0 μg/mL and 6.7 μg/mL, respectively. Lastly, at 24 h, K-562 presented the lowest IC<sub>50</sub> (5.3 μg/mL). After 72 h, the treatment with 5 μg/mL of oligomycin induced a metabolic inhibition on HEL, HL-60, and KG-1 cells higher than 50%, with HL-60 cells showing the lowest metabolic activity.

**Apoptosis as a mechanism of cell death activated by 2-DG and oligomycin**

We then evaluate the mechanism of cell death activated by 2-DG and oligomycin for the doses of 5 mM and 5 μg/mL, respectively, after 2 h (Supplemental Fig. 2) and 24 h (Fig. 3). After 24 h of incubation with 2-DG, the HEL cell line presented the highest percentage of cell death, mainly by apoptosis (Fig. 3a). In this cell line, incubation with 2-DG significantly decreased viable cells (27.6 ± 1.4%, *p* = 0.0008) and increased early apoptotic (43.4 ± 2.6%, *p* = 0.0008) and late apoptotic/necrotic cells (26.6 ± 2.8%, *p* = 0.0059) in comparison to untreated cells (viable: 89.4 ± 0.8%; early apoptosis: 4.2 ± 0.7%; late apoptosis/necrosis: 5.0 ± 0.7%). In HL-60, K-562, and NB-4 cell lines, cell viability decreased to 68.6 ± 3.7%, 77.4 ± 1.7%, and 83.8 ± 5.6%, respectively, and was accompanied by an increase in the percentage of cells in early apoptosis and late apoptosis/necrosis. Oligomycin treatment for 24 h significant decreased cell viability of HL-60 cells (45.0 ± 4.8%, *p* = 0.0011). This decrease was accompanied by an increase in the percentage of cells in early apoptosis (8.0 ± 1.1%, *p* = 0.0132), late apoptosis/necrosis (37.4 ± 6.1%, *p* = 0.0010), and necrosis (9.6 ± 3.9%, *p* = 0.0077) comparatively to untreated cells (viable: 88.0 ± 0.7%; early apoptosis: 3.6 ± 0.7%; late apoptosis/necrosis: 6.4 ± 0.2%; necrosis: 2.0 ± 0.3%). A cytotoxic effect was also observed in HEL

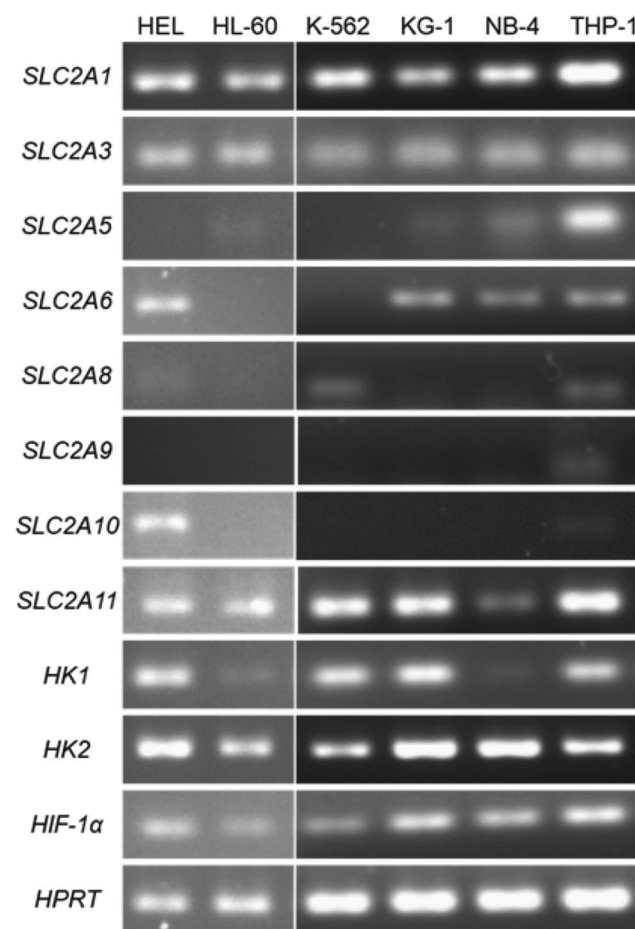


**Fig. 1** Metabolic-related gene expression in HEL, HL-60, K-562, KG-1, NB-4, and THP-1 cell lines. The expression of eight *SLC2A*, two *HK*, *HIF-1α*, and *HPRT* was assessed by RT-PCR as described in Methods. Data show the most representative bands of 3 independent experiments. *SLC2A* solute carrier family 2, *HK* hexokinase, *HIF-1α* hypoxia-inducible factor, *HPRT* hypoxanthine phosphoribosyltransferase

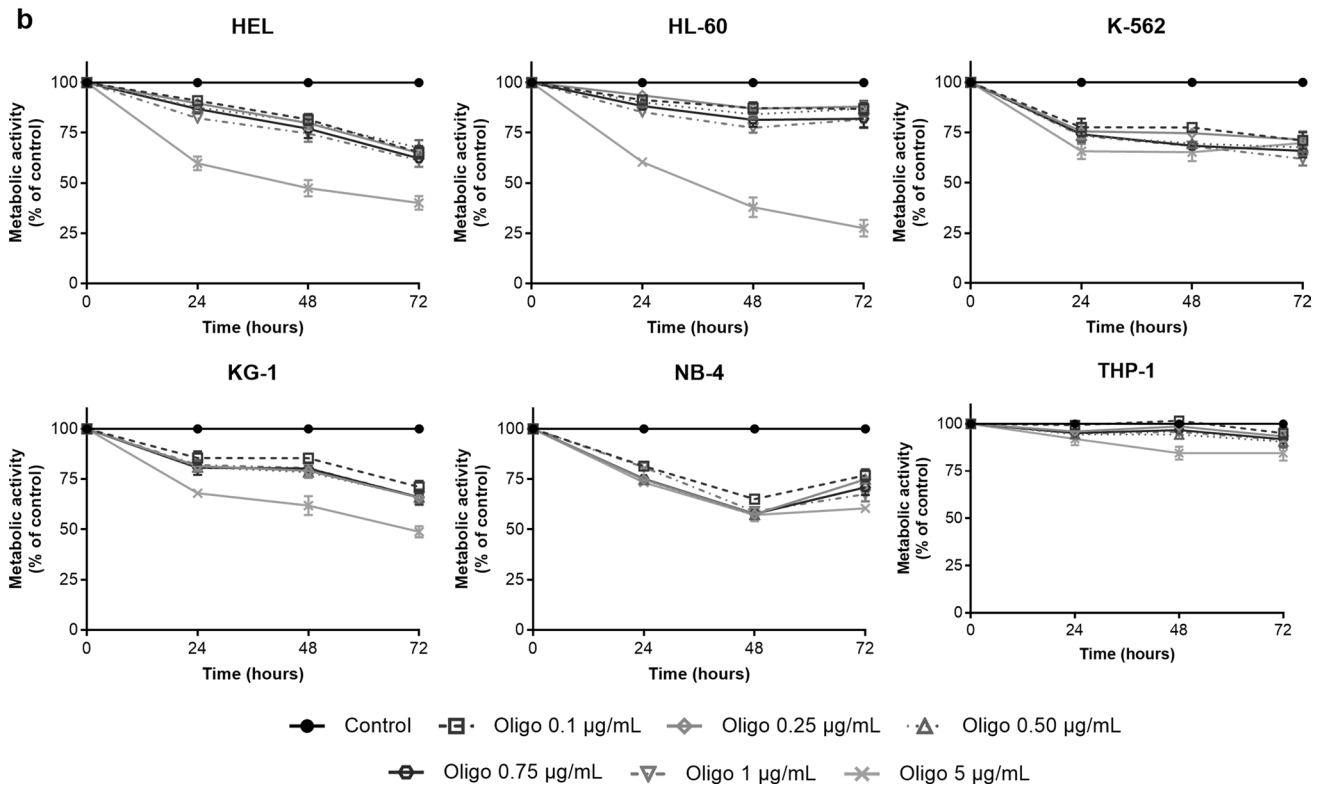
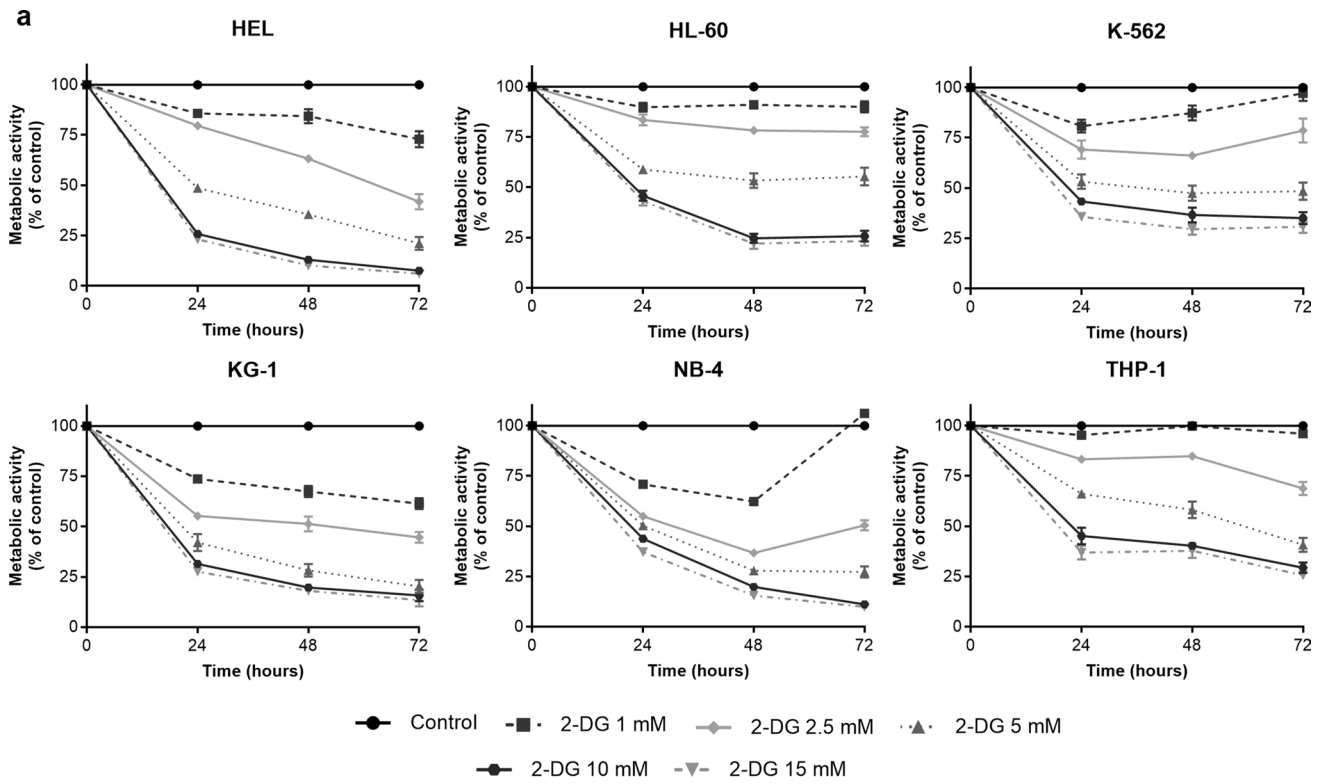


**Fig. 2** Dose–response curves of 2-deoxy-D-glucose (a) and oligomycin (b) in AML cell lines. Cells were cultured at optimal density and growth conditions in the absence (control) and in the presence of increasing doses of 2-DG or oligomycin for 72 h. At every 24 h, metabolic activity was assessed using a resazurin reduction assay, as described in Methods section. Results are expressed in percentage (%) normalized to control. Data are expressed as mean  $\pm$  SEM from 5 independent experiments. 2-DG 2-deoxy-D-glucose, *Oligo* oligomycin

and K-562, with a decrease of 31.2% and 13% of viable cells, respectively. In the KG-1 cell line, a decrease of viable cells after treatment with 2-DG (7.8% decrease) and oligomycin (9.2% decrease,  $p=0.0500$ ) was observed, mainly as a result of an increase of late apoptotic/necrotic cells. THP-1 cell viability remained similar to untreated cells (Fig. 3a). The morphological evaluation by optical microscopy showed typical features of cell death mediated by apoptosis (Fig. 3b). After treatment with 2-DG or oligomycin, the cells, particularly the ones with more cell death by FC, showed morphological aspects typical of apoptosis, like blebbing, nuclear fragmentation, and cellular contraction. Furthermore, it was possible to observe an increase in vacuolization on exposure cells, proving the toxicity induced by the drug.

### Cell cycle arrest in G<sub>0</sub>/G<sub>1</sub> phase promoted by 2-DG and oligomycin

Besides the cytotoxic effect, glycolysis and OXPHOS inhibitors can also induce a cytostatic effect on cells; therefore, the cell cycle distribution was evaluated, by FC, after 2 h (Supplemental Table S2) and 24 h of exposure to 2-DG and oligomycin (Table 2). Glycolysis inhibition by 2-DG arrested cells in the G<sub>0</sub>/G<sub>1</sub> phase in HEL ( $p=0.0171$ ), HL-60 ( $p=0.0377$ ) and KG-1 ( $p=0.0018$ ) cells. On the other hand, 2-DG treatment arrested THP-1 in the G<sub>2</sub>/M phase ( $p=0.0356$ ). Oligomycin induced a significant arrest in G<sub>0</sub>/G<sub>1</sub> phase in all cell lines (HEL:  $p=0.0138$ ; HL-60:  $p=0.056$ ; K-562:  $p=0.0121$ ; NB-4:  $p=0.0041$ ; THP-1:  $p=0.0017$ ), except in KG-1 cells where an increase of 15.4% of cells in this phase was observed. Additionally, the presence of an apoptotic peak (Sub-G<sub>1</sub>) was observed, corresponding to DNA fragmentation typical of apoptotic cells, particularly in the cell lines where more cell death was observed: HEL cells treated with 2-DG ( $p=0.0025$ ) and HL-60 cells treated with oligomycin ( $p=0.0012$ ) (Table 2), thus confirming the apoptosis induction in our previous studies (Fig. 3a).

### 2-DG and oligomycin alter <sup>18</sup>F-FDG uptake and metabolic genes expression levels

Glucose uptake after incubation with glycolysis and OXPHOS inhibitors, during 2 h (K-562) and 24 h, was

evaluated indirectly using <sup>18</sup>F-FDG. As shown in Fig. 4a, exposure to 2-DG led to a significant decrease in <sup>18</sup>F-FDG uptake. This decrease was more evident at 120 min in HEL (12.2-fold,  $p=0.0218$ ), KG-1 (4.5-fold), NB-4 (3.7-fold,  $p=0.0047$ ), and HL-60 (3.2-fold,  $p=0.0075$ ) cell lines. On the contrary, oligomycin resulted in a significant increase of <sup>18</sup>F-FDG uptake in K-562 cells (1.8-fold at 120 min,  $p=0.0471$ ), having little to no effect in the remaining cells.

Gene expression was evaluated by qPCR studies (5 *SLC2A* and 2 *HK*), after exposure to 2-DG and oligomycin for 2 h (Supplemental Fig. 3) and 24 h (Fig. 4b). 2-DG and oligomycin treatment increased *SLC2A1* expression levels in all cell lines in comparison to untreated cells, except in KG-1 cells. However, the results were significant in NB-4 (2-DG: twofold,  $p=0.0235$ ), HEL (2-DG: 1.9-fold,  $p=0.0235$ ; oligomycin: 4.7-fold,  $p=0.0079$ ), and HL-60 (2-DG: 1.4-fold,  $p=0.0154$ ; oligomycin: 1.7-fold,  $p=0.0124$ ). On the contrary in KG-1 cells, a decrease of the expression was observed (2-DG: 2.6-fold,  $p=0.0008$ ). Treatment with these inhibitors also increased *SLC2A5* expression levels, except for HL-60 (2-DG: twofold,  $p=0.0350$ ) and KG-1 (oligomycin: 1.6-fold,  $p=0.0287$ ). The increase was significant in HEL (2-DG: 8.3-fold,  $p=0.0235$ ; oligomycin: 9.6-fold,  $p=0.0079$ ) and K-562 cells (2-DG: 3.6-fold,  $p=0.0154$ ; oligomycin: 4.9-fold,  $p=0.0124$ ). Moreover, 2-DG increased *SLC2A9* expression levels in all cell lines, except in HL-60, with significance in HEL (4.4-fold,  $p=0.0235$ ) and NB-4 (3.9-fold,  $p=0.0154$ ). After OXPHOS inhibition, it was observed an increase in *SLC2A9* gene expression, mainly in NB-4 (6.3-fold,  $p=0.0124$ ), HEL (fivefold,  $p=0.0079$ ), K-562 (threefold,  $p=0.0024$ ), and HL-60 cells. This increase was not observed in KG-1 (Fig. 4b). 2-DG and oligomycin increased *SLC2A10* expression levels in THP-1 (2-DG: 4.4-fold,  $p=0.0079$ ; oligomycin: 3.7-fold,  $p=0.0235$ ), K-562 (oligomycin: 3.9-fold,  $p=0.0006$ ), and HEL cells (2-DG: 2.4-fold,  $p=0.0424$ ; oligomycin: 3.7-fold,  $p=0.0039$ ). 2-DG also significantly increased *SLC2A11* in KG-1 (2.5-fold,  $p=0.0006$ ), THP-1 (2.2-fold,  $p=0.0191$ ), NB-4 (twofold,  $p=0.0350$ ), and HEL cells (1.9-fold,  $p=0.0235$ ) and oligomycin in HEL (2.7-fold,  $p=0.0079$ ), HL-60 (2.3-fold,  $p=0.0011$ ), NB-4 (2.3-fold,  $p=0.0050$ ), K-562 (twofold,  $p=0.0008$ ), and THP-1 cells (1.9-fold,  $p=0.0100$ ). In all cell lines, except KG-1 (1.4-fold,  $p=0.0079$ ), *HK1* expression levels increased after treatment with oligomycin, being statistically significant in NB-4 (3.3-fold,  $p=0.0287$ ) and HL-60 (3.2-fold,  $p=0.0100$ ), when compared to untreated cells. 2-DG had a more variable effect, downregulating *HK1* expression in KG-1 (1.5-fold,  $p=0.0235$ ), HEL, and K-562 and upregulating in NB-4 (4.2-fold,  $p=0.0063$ ), THP-1 (2.6-fold,  $p=0.0024$ ), and HL-60 cells (1.9-fold,  $p=0.0191$ ). Lastly, both glycolysis and OXPHOS inhibition increased *HK2* expression levels in NB-4 (2-DG: 3.1-fold,  $p=0.0235$ ) and HL-60 cells (2-DG: 1.8-fold,  $p=0.0191$ ; oligomycin:

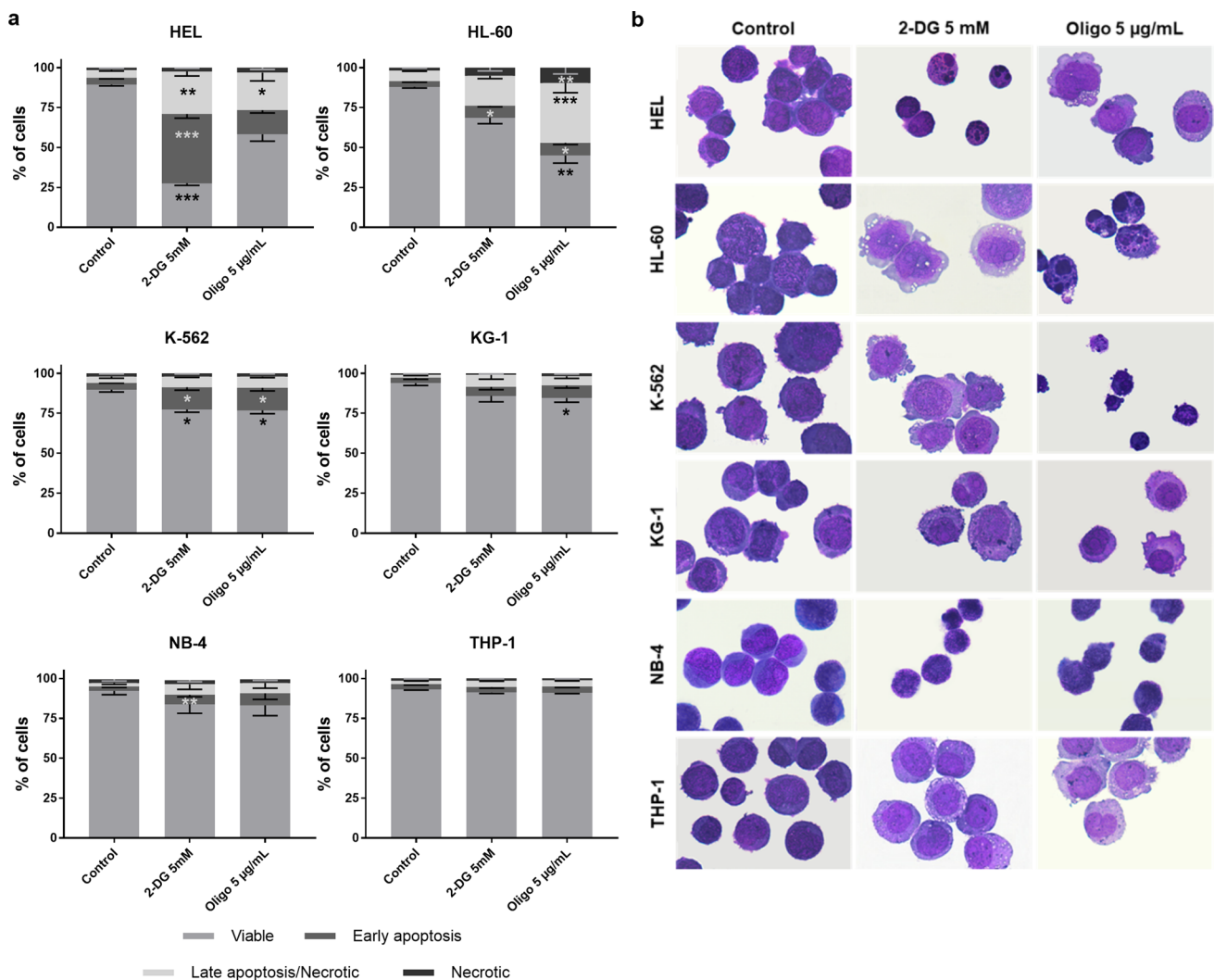


**Fig. 3** Analysis of cell death induced by 2-deoxy-D-glucose (5 mM) and oligomycin (5 µg/mL) in AML cell lines after 24 h of exposure. **(a)** Cell death was detected by annexin V/7-AAD double staining and analyzed by flow cytometry. Data are expressed as a percentage (%) of viable, early apoptosis, late apoptosis/necrotic, and necrotic cells and represent mean  $\pm$  SEM of 5 independent experiments. Statistical

analyses were performed by comparison with control, using Dunn's multiple comparisons test. **(b)** Cell morphology was observed by light microscopy using May-Grünwald-Giemsa staining (amplification: 1000  $\times$ ). The most representative image was selected. 2-DG 2-deoxy-D-glucose, *Oligo* oligomycin. \* $p < 0.05$ , \*\* $p < 0.01$  and \*\*\* $p < 0.001$

twofold,  $p = 0.0100$ ) and decreased in KG-1 (2-DG: 2.2-fold,  $p = 0.0063$ ; oligomycin: 1.7-fold,  $p = 0.0287$ ) and K-562 (2-DG: twofold,  $p = 0.0350$ ). *HK2* expression levels also decreased in HEL cells after treatment with 2-DG (1.7-fold,  $p = 0.0235$ ).

## Discussion

In our work, we demonstrate that 2-DG leads to a decrease in metabolic activity, inducing a cytotoxic and cytostatic effect, mostly in KG-1 and HEL cells. This treatment also decreased  $^{18}\text{F}$ -FDG uptake and increased *SLC2A* and *HK* gene expression levels. Regarding OXPHOS inhibition,

oligomycin treatment decreased metabolic activity in a very evident cell line-dependent manner. HL-60 was the most affected cell line, whereas THP-1 metabolic activity remained similar to untreated cells. Cell death by apoptosis and cell cycle arrest was observed after treatment, mainly in HL-60 cells.  $^{18}\text{F}$ -FDG uptake was not affected by the inhibition, except in K-562 cells where a decrease was observed. Interestingly, an increase of *SLC2A* and *HK* gene expression levels was observed.

The decrease of metabolic activity caused by 2-DG was first evident in KG-1 cells since, at 24 h, they required the lowest concentration to achieve  $\text{IC}_{50}$ . After 72 h, the sensitivity to this compound was also evident in HEL and NB-4 cells since they presented the lowest metabolic activity



**Table 2** Effects of 2-deoxy-D-glucose (5 mM) and oligomycin (5 µg/mL) in cell cycle distribution of AML cell lines after 24 h of treatment

		Sub-G <sub>1</sub> (%)	G <sub>0</sub> /G <sub>1</sub> (%)	S (%)	G <sub>2</sub> /M (%)
HEL	Control	1.0±0.4	57.2±2.0	33.0±2.2	9.4±0.7
	2-DG 5 mM	17.0±1.6**	66.2±1.0*	31.6±1.2	2.2±0.4**
	Oligo 5 µg/mL	9.2±2.9	66.4±1.3*	28.4±2.0	5.2±1.6
HL-60	Control	2.2±0.6	57.8±0.8	35.4±1.5	6.8±1.0
	2-DG 5 mM	11.0±2.2	72.2±1.3*	22.8±1.8*	5.0±0.7
	Oligo 5 µg/mL	43.0±4.6**	75.8±3.4**	21.0±2.8**	3.2±0.6*
K-562	Control	2.8±0.8	42.0±0.9	49.4±2.4	9.6±2.3
	2-DG 5 mM	3.0±0.5	46.0±2.2	46.8±1.5	8.0±1.4
	Oligo 5 µg/mL	3.0±0.9	49.2±1.2*	40.8±0.7*	10.8±1.2
KG-1	Control	0.6±0.4	41.0±2.5	38.4±2.3	20.4±1.3
	2-DG 5 mM	1.2±0.6	64.2±3.0**	27.0±2.3*	8.8±0.9**
	Oligo 5 µg/mL	1.4±0.4	56.4±2.7	32.6±2.5	11.0±1.3*
NB-4	Control	0.8±0.6	49.8±2.1	36.0±1.2	14.2±2.8
	2-DG 5 mM	3.8±3.1	52.4±1.4	42.0±1.8	5.6±1.7
	Oligo 5 µg/mL	4.2±2.5	70.8±1.9**	22.4±1.4	7.8±1.1
THP-1	Control	0.8±0.4	48.8±1.9	45.4±2.9	5.6±1.2
	2-DG 5 mM	0.6±0.4	66.8±2.7	23.4±2.4	10.0±1.0*
	Oligo 5 µg/mL	1.6±0.5	74.6±1.7**	17.6±1.3**	7.8±0.8

Data are expressed as percentage of each cell cycle phase and represent mean ± SEM obtained from 5 independent experiments. Statistical analyses were performed by comparison with control, using Dunn’s multiple comparisons test

2-DG 2-deoxy-D-glucose, Oligo oligomycin

\**p* < 0.05 and \*\**p* < 0.01

values, similar to those observed for KG-1. These results could suggest a greater dependence on glycolysis by these cell lines. On the other hand, THP-1 and HL-60 cells were the most resistant, needing around 2.5-fold more 2-DG than KG-1. A study conducted by Suganuma et al. also observed that THP-1 and HL-60 cell lines are relatively resistant to 2-DG [17]. This is consistent with previous reports that showed that THP-1 cells might depend more on fatty acid oxidation for energy production [20], whereas HL-60 cell line may be dependent on glutamine metabolism [21]. Earlier studies showed that cells treated with moderate concentrations of 2-DG under normoxia conditions undergo growth inhibition instead of cell death since cells still produce ATP through their mitochondria using alternative energy sources [22, 23]. Such inhibition was also observed in our study, due to an increase of cells in G<sub>0</sub>/G<sub>1</sub> phase, being more evident in KG-1 cells, but also in HEL and HL-60. 2-DG inhibits cell growth by lowering cyclin D1 levels, a relevant cyclin in the transition of G<sub>0</sub>/G<sub>1</sub> to S phase of cell cycle. On account of that, an increase of cells in G<sub>0</sub>/G<sub>1</sub> phase is observed [22, 24], as in this study. However, Kurtoglu et al. showed that glycolytic inhibitors could become toxic if cells carry mitochondrial defects, even under normoxic conditions, leading to cell death [25]. The cytotoxic effect of 2-DG was predominantly evident in the HEL cell line, where a significant increase of apoptotic cells was observed. These cells

carry the *JAK2*<sup>V617F</sup> mutation [26]. This mutation induces ROS accumulation [27], and high levels of ROS could be an indicator of mitochondrial defects. Therefore, the high death observed in HEL cells could result from mitochondrial dysfunctions, since these cells presented the highest basal levels of peroxides and superoxide anion.

Cells can obtain energy by several metabolic pathways; therefore, the inhibition of glycolysis could be associated with changes on cell metabolic profile. Glycolysis inhibition decreased <sup>18</sup>F-FDG uptake in HEL, HL-60, NB-4, and KG-1 cells, being more evident in HEL. 2-DG undergoes facilitated diffusion into cells via GLUTs and once inside the cells, it is phosphorylated by HK, with formation of 2-DG-6-phosphate (2-DG-6-P), which is not metabolized blocking the glycolytic pathway [4, 28]. Cancer cells that have higher demand for glucose will have a greater 2-DG uptake and therefore a higher 2-DG-6-P accumulation [29]. Such accumulation could lead to a negative feedback regulation that would prevent glucose, and by analogy <sup>18</sup>F-FDG, from entering the cell. Hence, our results suggest that HEL cell line is the most dependent on glucose uptake. This fact is also supported by the high baseline uptake of <sup>18</sup>F-FDG. On the contrary, THP-1 cells did not seem to need high levels of glucose, as they present low levels of <sup>18</sup>F-FDG uptake. However, THP-1 in addition to expressing all the tested *SLC2A* genes showed the

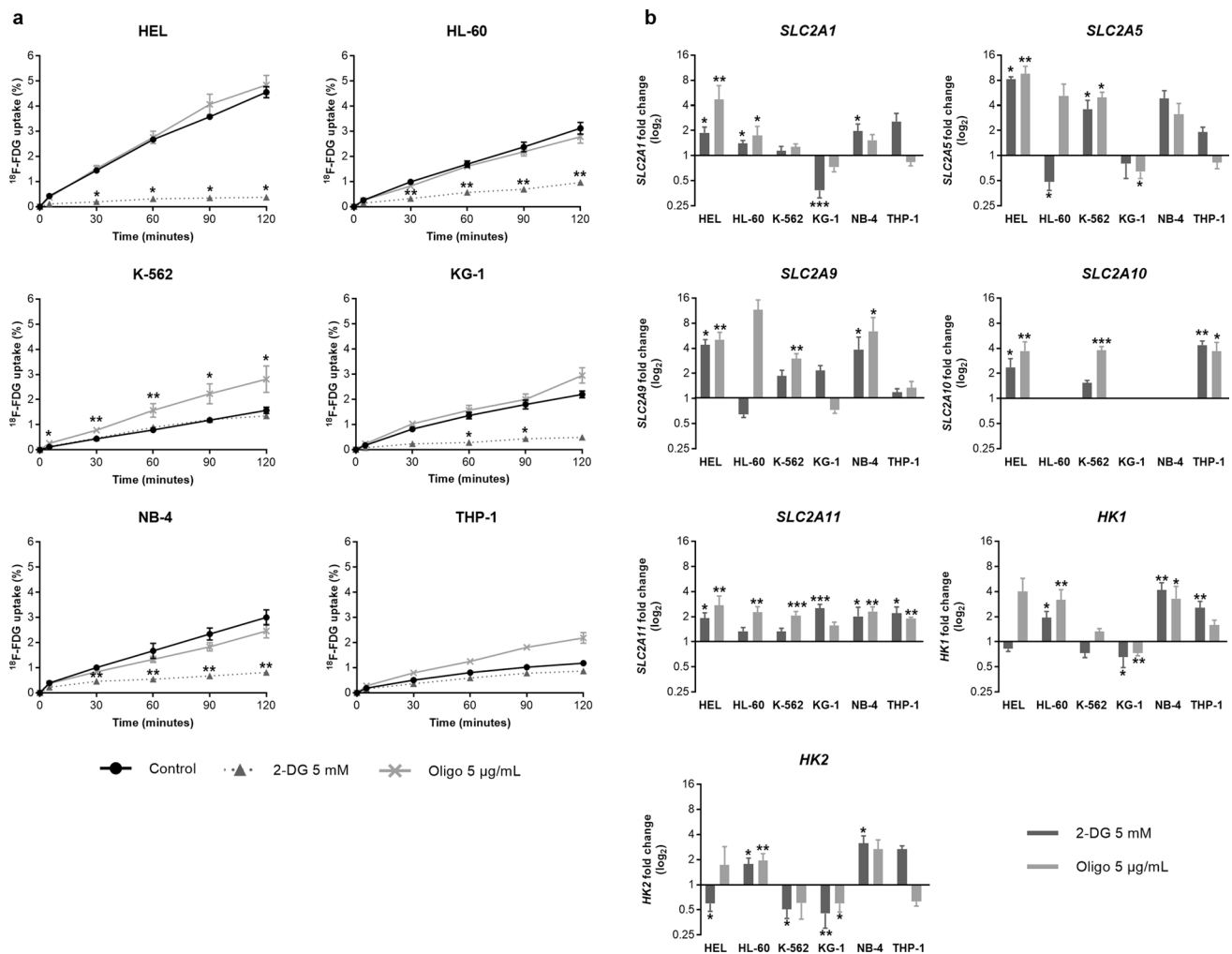


**Fig. 4** Modulation of  $^{18}\text{F}$ -FDG uptake and metabolic-related gene expression by 2-deoxy-D-glucose and oligomycin in AML cell lines. **(a)**  $^{18}\text{F}$ -FDG uptake profile of AML cell lines after exposure to 2-DG (5 mM) and oligomycin (5  $\mu\text{g}/\text{mL}$ ) during 2 h (K-562) or 24 h, as described in Methods.  $^{18}\text{F}$ -FDG uptake was assessed after 5, 30, 60, 90, and 120 min of incubation. Data are expressed in percentage (%) and represent mean  $\pm$  SEM of 5 independent experiments. **(b)** Gene expression levels of five *SLC2A* and two *HK* in AML cell lines were quantified by qPCR after treatment with 2-DG (5 mM) and oligomy-

cin (5  $\mu\text{g}/\text{mL}$ ) for 24 h. The continuous black line in the figure represents the expression levels in untreated control cells. Results are normalized to the *HPRT* gene, and data are expressed as mean  $\pm$  SEM from 5 independent experiments. Statistical analyses were performed by comparison with control, using Dunn's multiple comparisons test. 2-DG 2-deoxy-D-glucose, *Oligo* oligomycin; *SLC2A* solute carrier family 2, *HK* hexokinase, *HPRT* hypoxanthine phosphoribosyltransferase. \* $p < 0.05$ , \*\* $p < 0.01$  and \*\*\* $p < 0.001$

higher basal expression levels of these genes. Hence, the high and diversified expression of these genes could be a compensatory mechanism due to changes in metabolic pathways. The observation that THP-1 has low  $^{18}\text{F}$ -FDG uptake is consistent with previous reports showing that THP-1 appears to use an alternative energy source other than glucose [17, 20]. Considering that  $^{18}\text{F}$ -FDG enters the cells by GLUTs, in particular GLUT1 and GLUT3, encoded by *SLC2A1* and *SLC2A3* genes, respectively, it would be expected that a decrease in  $^{18}\text{F}$ -FDG uptake would be accompanied by a decrease of *SLC2A* expression levels. Our results, except in punctual cases, show

an increase in *SLC2A* gene expression levels. However, it is important to point out that the GLUTs protein levels were not assessed, and their levels could affect  $^{18}\text{F}$ -FDG uptake. Since 2-DG competitively inhibits GLUTs [29], the increase of *SLC2A* expression levels observed could be the result of a compensatory mechanism. The *SLC2A10* gene, that encodes GLUT10, was only found expressed in HEL, K-562, and THP-1 cells. GLUT10 exhibits a very low intrinsic transport activity [30, 31], thus having little effect on  $^{18}\text{F}$ -FDG uptake. Further, in cells treated with 2-DG, a decrease of *HK1* and *HK2* expression levels in HEL, K-562, and KG-1 erythroleukemia cell lines, and an

increase in HL-60, NB-4, and THP-1 are observed, suggesting a relation between these changes in *HK* expression levels and AML subtypes.

OXPPOS inhibition reduced the metabolic activity in all cell lines, except in THP-1 where an  $IC_{50}$  of 44.8  $\mu\text{g}/\text{mL}$  was estimated, being by far the cells most resistant to OXPPOS inhibition. After 24 h of exposure, K-562 cells were the most affected by oligomycin. However, after 72 h, HL-60 cells showed the lowest metabolic activity after treatment with the highest tested dose, being the most affected by this inhibition. This suggests a higher dependency on this metabolic pathway. THP-1 cells did not seem to depend on OXPPOS for energy production. Though, Sukanuma et al. showed that THP-1 cell line, which was relatively resistant to 2-DG, as in this study, was sensitive to oligomycin, and, therefore, was considered to depend on OXPPOS for energy production, in particular fatty acid oxidation, as previously stated [17, 20]. Oligomycin complex is an inhibitor of mitochondrial  $F_1F_0$ -ATP synthase, thus inhibiting the production of ATP [32]. Reduction of ATP levels is one of the apoptosis triggers [33, 34], therefore, cell lines that depend more on this mechanism to obtain energy will have a higher decrease of ATP production that could result in high levels of death. The cytotoxic effect of OXPPOS inhibition was mainly observed in HL-60 cells that showed increased apoptotic cells. This cell line carries *MYC* gene amplification that induces mitochondrial metabolism and, especially, glutamine metabolism [6]. A previous study considered glutamine the main energy source for HL-60 cells [21], which could explain why this cell line presented more cell death. Some cytotoxic effect was also observed in erythroleukemia cell lines (HEL, K-562, and KG-1), and apoptosis in this AML subtype after incubation with oligomycin was already observed by others [34]. However, the cytostatic effect appeared to be the main result of OXPPOS inhibition, arresting cells in  $G_0/G_1$  phase in almost all tested cells. These results are in agreement with studies showing that oligomycin induces cell cycle arrest by suppressing cyclin D1 and B1 expression levels, resulting in  $G_1$  phase arrest [24, 35]. OXPPOS inhibition had a cytotoxic and cytostatic effect on HL-60 cells, which could again suggest a dependency of this cell line for this pathway. The cell cycle arrest in  $G_1$  phase induced by oligomycin in HL-60 cells was also observed by a previous study [35]. OXPPOS inhibition results in fewer ATP production, hence cancer cells need to compensate by resorting to another metabolic pathway, such as glycolysis. OXPPOS inhibition led to a significant increase in *SLC2A* expression levels, which could be a way for the cells to intensify glucose uptake. However, when  $^{18}\text{F}$ -FDG uptake was assessed, this increase was only observed in K-562 cells. In HL-60 cells, *MYC* increases glutamine uptake [6] and therefore,

moderate concentrations of oligomycin may not affect glucose but, preferentially, glutamine uptake. The preference for glutamine uptake over glucose could also explain why this cell line presented the lowest *SLC2A* expression levels. Additionally, oligomycin also increased *HK* expression. Considering that metabolic reprogramming is associated with GLUTs and HK overexpression, an increase in expression levels of these genes after OXPPOS inhibition could indicate a metabolic shift towards glycolysis. The variant found in *IDH1* exon 4 (rs11554137) of HEL, HL-60, K-562 and KG-1 cells lies near the R132 mutational hotspot and their detection is mutually exclusive in relation to *IDH1*<sup>R132</sup> mutations. Although considered benign in ClinVar database, this variant was reported to be associated with poor prognosis in adult AML patients cytogenetically normal [36–38]. In this study, we do not find a correlation between this genetic variant in *IDH1* and the response to 2-DG or oligomycin.

In conclusion, although cancer is usually more associated with a glycolytic phenotype, this work showed that not all cancer cells depend on this metabolic pathway in the same way. The six AML cell lines used seem to have different metabolic profiles and different responses to metabolic inhibitors. All the tested cell lines appeared to depend on glycolysis. However, HEL and KG-1 showed greater dependence with higher glucose consumption and sensitivity to glycolysis inhibition. On the other hand, THP-1 was the least dependent on lower glucose uptake and higher resistance to glycolysis inhibition. THP-1 did not seem to be dependent on OXPPOS, whereas HL-60 cells were the most dependent on this pathway, showing high sensitivity and cell death/cell cycle arrest. To suppress OXPPOS inhibition, cells seem to reprogram their metabolism, which could suggest that glycolysis may be a better therapeutic target in AML. However, these results suggest that targeting only one metabolic pathway may not be enough since there are alternative pathways to overcome glycolysis inhibition.

**Acknowledgements** The present work was supported by Center of Investigation on Environment, Genetics and Oncobiology (CIMAGO), Faculty of Medicine, University of Coimbra, Portugal and by National Funds via Foundation for Science and Technology (FCT) through the Strategic Project UID/NEU/04539/2019, COMPETE-FEDER (POCI-01-0145-FEDER-007440), UIDB/04539/2020, and UIDP/04539/2020 (CIBB). RA was supported by FCT through a PhD Grant (SFRH/BD/51994/2012).

**Author contributions** ACG and ABSR designed the experiments. BL and ACG drafted the manuscript. BL, ACG, RA, JJ, ASP, AMA, AA, MFB, and MC performed or interpreted the experiments. BL, JJ, and RA executed the statistical analyses. JMNC and ABSR revised the manuscript.

**Funding** The present work was supported by the Center of Investigation on Environment, Genetics and Oncobiology (CIMAGO), Faculty of Medicine, University of Coimbra, Portugal and by National Funds

via Foundation for Science and Technology (FCT) through the Strategic Project UID/NEU/04539/2019, COMPETE-FEDER (POCI-01-0145-FEDER-007440), UIDB/04539/2020, and UIDP/04539/2020 (CIBB). RA was supported by the Portuguese Foundation to Science and Technology (FCT) through a PhD Grant (SFRH/BD/51994/2012).

**Data availability** The data used and/or analyzed during the current study are available by contacting the corresponding author with reasonable request.

## Compliance with ethical standards

**Conflict of interest** The authors declare no conflicts of interests.

**Ethical approval** This research project was approved by the Institutional Review Board of the Medical School of the University of Coimbra (reference: 072-CE-2017).

**Consent to participate** Not applicable.

**Consent for publication** The authors declare that they consent to the manuscript publication.

## References

- Ghaffari P, Mardinoglu A, Nielsen J. Cancer metabolism: a modeling perspective. *Front. Physiol.* 2015;6:382. <https://doi.org/10.3389/fphys.2015.00382>.
- Schulze A, Harris AL. How cancer metabolism is tuned for proliferation and vulnerable to disruption. *Nature.* 2012;491(7424):364–73. <https://doi.org/10.1038/nature11706>.
- Koppenol WH, Bounds PL, Dang CV. Otto Warburg's contributions to current concepts of cancer metabolism. *Nat Rev Cancer.* 2011;11(5):325–37. <https://doi.org/10.1038/nrc3038>.
- Kalyanaraman B. Teaching the basics of cancer metabolism: Developing antitumor strategies by exploiting the differences between normal and cancer cell metabolism. *Redox Biol.* 2017;12:833–42. <https://doi.org/10.1016/j.redox.2017.04.018>.
- Warburg O. On the origin of cancer cells. *Science.* 1956;123(3191):309–14. <https://doi.org/10.1126/science.123.3191.309>.
- Cairns RA, Harris IS, Mak TW. Regulation of cancer cell metabolism. *Nat Rev Cancer.* 2011;11(2):85–95. <https://doi.org/10.1038/nrc2981>.
- Zheng J. Energy metabolism of cancer: glycolysis versus oxidative phosphorylation (review). *Oncol Lett.* 2012;4(6):1151–7. <https://doi.org/10.3892/ol.2012.928>.
- Pavlova NN, Thompson CB. The emerging hallmarks of cancer metabolism. *Cell Metab.* 2016;23(1):27–47. <https://doi.org/10.1016/j.cmet.2015.12.006>.
- Yeung SJ, Pan J, Lee MH. Roles of p53, MYC and HIF-1 in regulating glycolysis: the seventh hallmark of cancer. *Cell Mol Life Sci CMLS.* 2008;65(24):3981–99. <https://doi.org/10.1007/s00018-008-8224-x>.
- Courtney R, Ngo DC, Malik N, Verweris K, Tortorella SM, Karagiannis TC. Cancer metabolism and the Warburg effect: the role of HIF-1 and PI3K. *Mol Biol Rep.* 2015;42(4):841–51. <https://doi.org/10.1007/s11033-015-3858-x>.
- Danhier P, Banski P, Payen VL, Grasso D, Ippolito L, Sonveaux P, et al. Cancer metabolism in space and time: beyond the Warburg effect. *Biochem Biophys Acta.* 2017;1858(8):556–72. <https://doi.org/10.1016/j.bbabi.2017.02.001>.
- Hagland H, Nikolaisen J, Hodneland LI, Gjertsen BT, Brusserud O, Tronstad KJ. Targeting mitochondria in the treatment of human cancer: a coordinated attack against cancer cell energy metabolism and signalling. *Expert Opin Ther Targets.* 2007;11(8):1055–69. <https://doi.org/10.1517/14728222.11.8.1055>.
- Prada-Arismendy J, Arroyave JC, Rothlisberger S. Molecular biomarkers in acute myeloid leukemia. *Blood Rev.* 2017;31(1):63–766. <https://doi.org/10.1016/j.blre.2016.08.005>.
- Chan SM, Majeti R. Role of DNMT3A, TET2, and IDH1/2 mutations in pre-leukemic stem cells in acute myeloid leukemia. *Int J Hematol.* 2013;98(6):648–57. <https://doi.org/10.1007/s12185-013-1407-8>.
- Sun Y, Chen BR, Deshpande A. Epigenetic regulators in the development, maintenance, and therapeutic targeting of acute myeloid leukemia. *Front Oncol.* 2018;8:41. <https://doi.org/10.3389/fonc.2018.00041>.
- Eriksson A, Lennartsson A, Lehmann S. Epigenetic aberrations in acute myeloid leukemia: early key events during leukemogenesis. *Exp Hematol.* 2015;43(8):609–24. <https://doi.org/10.1016/j.exphem.2015.05.009>.
- Suganuma K, Miwa H, Imai N, Shikami M, Gotou M, Goto M, et al. Energy metabolism of leukemia cells: glycolysis versus oxidative phosphorylation. *Leuk Lymphoma.* 2010;51(11):2112–9. <https://doi.org/10.3109/10428194.2010.512966>.
- Jorge J, Petronilho S, Alves R, Coucelo M, Goncalves AC, Nascimento Costa JM, et al. Apoptosis induction and cell cycle arrest of pladienolide B in erythroleukemia cell lines. *Investig New Drugs.* 2020;38(2):369–77. <https://doi.org/10.1007/s10637-019-00796-2>.
- Brito AF, Abrantes AM, Ribeiro M, Oliveira R, Casalta-Lopes J, Goncalves AC, et al. Fluorine-18 fluorodeoxyglucose uptake in hepatocellular carcinoma: correlation with glucose transporters and p53 expression. *J Clin Exp Hepatol.* 2015;5(3):183–9. <https://doi.org/10.1016/j.jceh.2015.05.003>.
- Miwa H, Shikami M, Goto M, Mizuno S, Takahashi M, Tsunekawa-Imai N, et al. Leukemia cells demonstrate a different metabolic perturbation provoked by 2-deoxyglucose. *Oncol Rep.* 2013;29(5):2053–7. <https://doi.org/10.3892/or.2013.2299>.
- Goto M, Miwa H, Shikami M, Tsunekawa-Imai N, Suganuma K, Mizuno S, et al. Importance of glutamine metabolism in leukemia cells by energy production through TCA cycle and by redox homeostasis. *Cancer Invest.* 2014;32(6):241–7. <https://doi.org/10.3109/07357907.2014.907419>.
- Liu H, Kurtoglu M, Cao Y, Xi H, Kumar R, Axten JM, et al. Conversion of 2-deoxyglucose-induced growth inhibition to cell death in normoxic tumor cells. *Cancer Chemother Pharmacol.* 2013;72(1):251–62. <https://doi.org/10.1007/s00280-013-2193-y>.
- Xi H, Kurtoglu M, Liu H, Wangpaichitr M, You M, Liu X, et al. 2-Deoxy-D-glucose activates autophagy via endoplasmic reticulum stress rather than ATP depletion. *Cancer Chemother Pharmacol.* 2011;67(4):899–910. <https://doi.org/10.1007/s00280-010-1391-0>.
- Xiong W, Jiao Y, Huang W, Ma M, Yu M, Cui Q, et al. Regulation of the cell cycle via mitochondrial gene expression and energy metabolism in HeLa cells. *Acta Biochim Biophys Sin.* 2012;44(4):347–58. <https://doi.org/10.1093/abbs/gms006>.
- Kurtoglu M, Gao N, Shang J, Maher JC, Lehrman MA, Wangpaichitr M, et al. Under normoxia, 2-deoxy-D-glucose elicits cell death in select tumor types not by inhibition of glycolysis but by interfering with N-linked glycosylation. *Mol Cancer Ther.* 2007;6(11):3049–58. <https://doi.org/10.1158/1535-7163.MCT-07-0310>.
- Quentmeier H, MacLeod RA, Zaborski M, Drexler HG. JAK2 V617F tyrosine kinase mutation in cell lines derived from myeloproliferative disorders. *Leukemia.* 2006;20(3):471–6. <https://doi.org/10.1038/sj.leu.2404081>.



27. Marty C, Lacout C, Droin N, Le Couedic JP, Ribrag V, Solary E, et al. A role for reactive oxygen species in JAK2 V617F myeloproliferative neoplasm progression. *Leukemia*. 2013;27(11):2187–95. <https://doi.org/10.1038/leu.2013.102>.
28. Seo M, Crochet RB, Lee Y-H. Targeting altered metabolism-emerging cancer therapeutic. *Strategies*. 2014;12:427–48. <https://doi.org/10.1016/b978-0-12-396521-9.00014-0>.
29. Zhang D, Li J, Wang F, Hu J, Wang S, Sun Y. 2-Deoxy-D-glucose targeting of glucose metabolism in cancer cells as a potential therapy. *Cancer Lett*. 2014;355(2):176–83. <https://doi.org/10.1016/j.canlet.2014.09.003>.
30. Mueckler M, Thorens B. The SLC2 (GLUT) family of membrane transporters. *Mol Aspects Med*. 2013;34(2–3):121–38. <https://doi.org/10.1016/j.mam.2012.07.001>.
31. Calvo MB, Figueroa A, Pulido EG, Campelo RG, Aparicio LA. Potential role of sugar transporters in cancer and their relationship with anticancer therapy. *Int J Endocrinol*. 2010. <https://doi.org/10.1155/2010/205357>.
32. Nagle DG, Zhou Y-D. Natural products as probes of selected targets in tumor cell biology and hypoxic signaling. In: Liu H-W, Mander L, editors. *Comprehensive natural products II*. Oxford: Elsevier; 2010. p. 651–683.
33. Shchepina LA, Pletjushkina OY, Avetisyan AV, Bakeeva LE, Fetisova EK, Izyumov DS, et al. Oligomycin, inhibitor of the F<sub>0</sub> part of H<sup>+</sup>-ATP-synthase, suppresses the TNF-induced apoptosis. *Oncogene*. 2002;21(53):8149–57. <https://doi.org/10.1038/sj.onc.1206053>.
34. Comelli M, Di Pancrazio F, Mavelli I. Apoptosis is induced by decline of mitochondrial ATP synthesis in erythroleukemia cells. *Free Radic Biol Med*. 2003;34(9):1190–9. [https://doi.org/10.1016/S0891-5849\(03\)00107-2](https://doi.org/10.1016/S0891-5849(03)00107-2).
35. Gemin A, Sweet S, Preston TJ, Singh G. Regulation of the cell cycle in response to inhibition of mitochondrial generated energy. *Biochem Biophys Res Commun*. 2005;332(4):1122–32. <https://doi.org/10.1016/j.bbrc.2005.05.061>.
36. Ho PA, Kopecky KJ, Alonzo TA, Gerbing RB, Miller KL, Kuhn J, et al. Prognostic implications of the IDH1 synonymous SNP rs11554137 in pediatric and adult AML: a report from the Children's Oncology Group and SWOG. *Blood*. 2011;118(17):4561–6. <https://doi.org/10.1182/blood-2011-04-348888>.
37. Xu Q, Li Y, Lv N, Jing Y, Xu Y, Li W, et al. Correlation between isocitrate dehydrogenase gene aberrations and prognosis of patients with acute myeloid leukemia: a systematic review and meta-analysis. *Clin Cancer Res*. 2017;23(15):4511–22. <https://doi.org/10.1158/1078-0432.CCR-16-2628>.
38. Willander K, Falk IJ, Chaireti R, Paul E, Hermansson M, Green H, et al. Mutations in the isocitrate dehydrogenase 2 gene and IDH1 SNP 105C>T have a prognostic value in acute myeloid leukemia. *Biomark Res*. 2014;2:18. <https://doi.org/10.1186/2050-7771-2-18>.

**Publisher's Note** Springer Nature remains neutral with regard to jurisdictional claims in published maps and institutional affiliations.